Cell Stem Cell

Supplemental Information

The *Dlk1-Gtl2* Locus Preserves LT-HSC Function by Inhibiting the PI3K-mTOR Pathway to Restrict Mitochondrial Metabolism

Pengxu Qian, Xi C. He, Ariel Paulson, Zhenrui Li, Fang Tao, John M. Perry, Fengli Guo, Meng Zhao, Lei Zhi, Aparna Venkatraman, Jeffrey S. Haug, Tari Parmely, Hua Li, Rick T. Dobrowsky, Wen-Xing Ding, Tomohiro Kono, Anne C. Ferguson-Smith, and Linheng Li

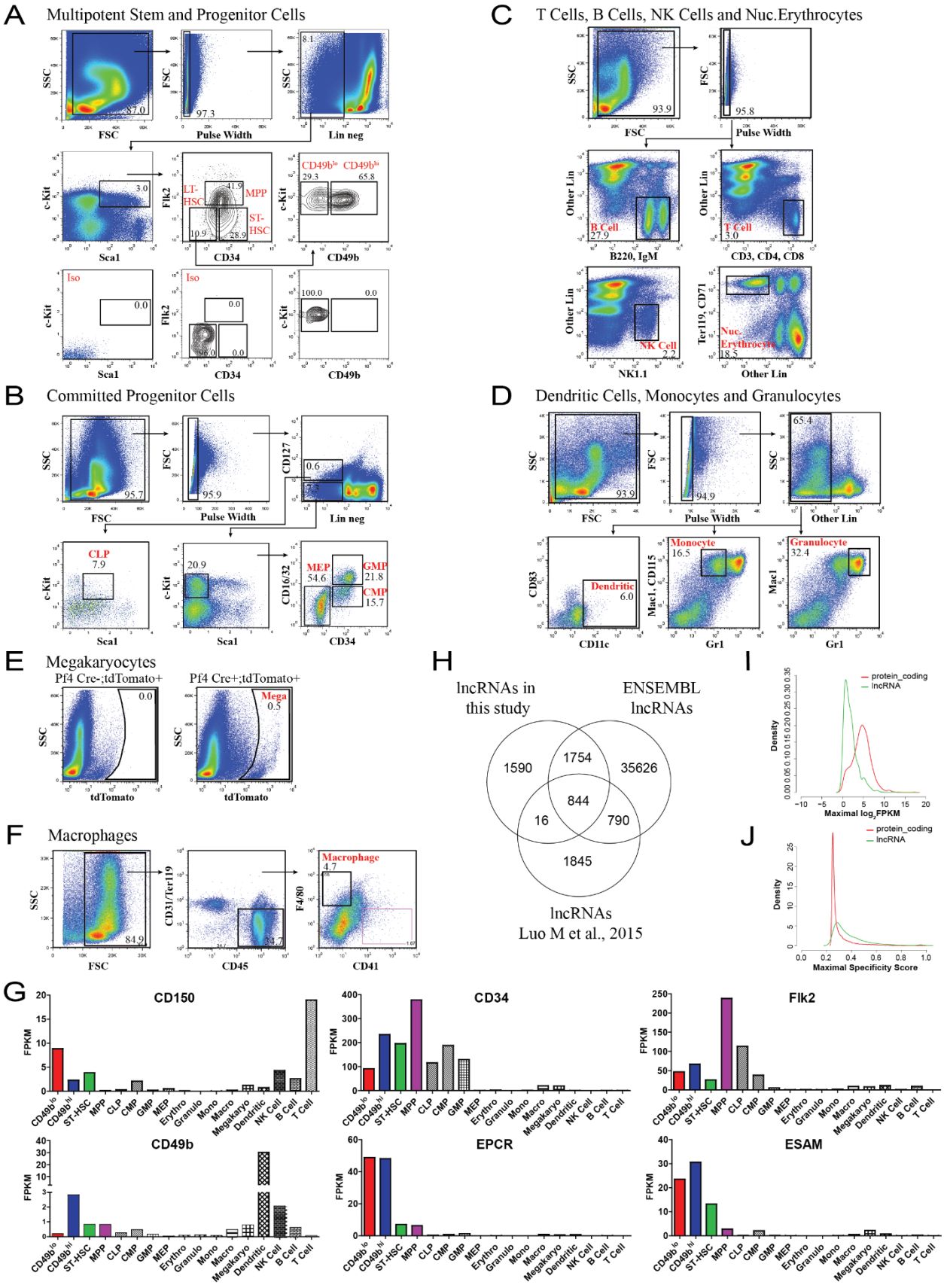
A
Multipotent Stem and Progenitor Cells
SSC
FSC
97.0
FSC
Pulse Width
97.3
SSC
Lin neg
8.1
c-Kit
Sca1
3.0
Flk2
CD34
LT-HSC
MPP
ST-HSC
41.9
10.9
28.9
c-Kit
CD49b
CD49b^lo
CD49b^hi
29.3
65.8
Iso
0.0
96.0
100.0
B
Committed Progenitor Cells
95.7
95.9
CD127
0.6
23.3
CLP
7.9
20.9
CD16/32
MEP
54.6
GMP
21.8
CMP
15.7
C
T Cells, B Cells, NK Cells and Nuc.Erythrocytes
93.9
95.8
Other Lin
B Cell
27.9
B220, IgM
T Cell
3.0
CD3, CD4, CD8
NK Cell
2.2
NK1.1
Ter119, CD71
Nuc. Erythrocyte
18.5
D
Dendritic Cells, Monocytes and Granulocytes
93.9
94.9
65.4
Other Lin
CD83
Dendritic
6.0
CD11c
Mac1, CD115
Monocyte
16.5
Gr1
Granulocyte
32.4
Mac1
E
Megakaryocytes
Pf4 Cre-;tdTomato+
Pf4 Cre+;tdTomato+
0.0
Mega
0.5
tdTomato
F
Macrophages
84.9
CD31/Ter119
34.7
CD45
Macrophage
4.7
F4/80
CD41
H
lncRNAs in this study
ENSEMBL lncRNAs
1590
1754
35626
844
16
790
1845
lncRNAs Luo M et al., 2015
I
protein_coding
lncRNA
Density
Maximal log2FPKM
J
protein_coding
lncRNA
Density
Maximal Specificity Score
G
CD150
CD34
Flk2
CD49b
EPCR
ESAM
FPKM
CD49b^lo
CD49b^hi
ST-HSC
MPP
CLP
CMP
GMP
MEP
Erythro
Granulo
Mono
Macro
Megakaryo
Dendritic
NK Cell
B Cell
T Cell

Figure S1. FACS Plots Showing the Strategy to Purify the 17 Hematopoietic Cell Populations Analyzed in This Study, Related to Figure 1. (**A**) Multipotent stem and progenitor cells, including CD49b^{lo} LT-HSCs, CD49b^{hi} IT-HSCs, ST-HSC and MPP cells, from C57BL/6 mice. (**B**) Committed progenitor cells, including CMP, GMP, MEP and CLP cells, from C57BL/6 mice. (**C**) Mature T cells, B cells, NK cells and nucleated erythrocytes from C57BL/6 mice. (**D**) Mature dendritic cells, monocytes and granulocytes from C57BL/6 mice. (**E**) Mature megakaryocytes from *Pf4-cre*$^{+}$*;R26R*^{tdTomato} mice. (**F**) Mature macrophages from C57BL/6 mice. (**G**) RNA-seq analysis of known HSC markers and the markers used for FACS in 17 hematopoietic cell types. (**H**) Venn diagram shows the overlaps among lncRNAs annotated in Ensembl databases, reported in a recent study (Luo et al., 2015) and identified in this study. (**I**) LncRNAs have overall lower expression than protein-coding genes. Maximal FPKM counts (log_2-normalized) of each lncRNA (green, n=1693) and coding (red, n=13775) transcript. (**J**) Cell specificity of RNAs according to type. Shown are distributions of maximal cell specificity scores calculated for each transcript from the RNA seq data for lncRNA (green, n=1693) and coding (red, n=13775).

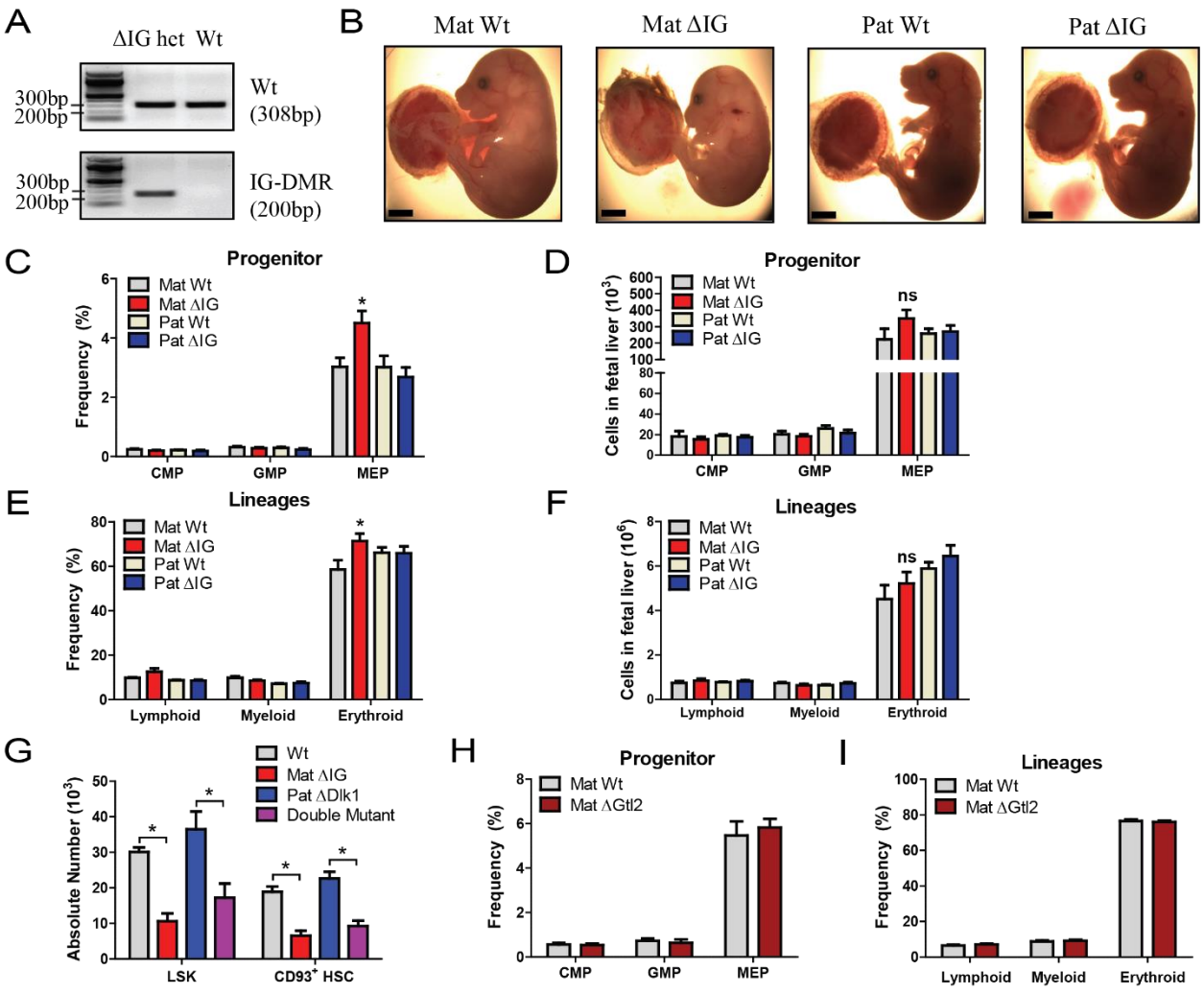

Figure S2. Loss of Imprinting at *Dlk1-Gtl2* Locus Did Not Affect Progenitors and Mature Lineage Cells in Fetal Liver, Related to Figure 2. (**A**) Electrophoresis patterns of PCR genotyping products from wt and *ΔIG* E15 embryo tails. (**B**) Gross phenotype of E15 wt littermate and *ΔIG* mutant embryos. (**C** and **D**) Frequency in TNC (C) and absolute numbers (D) of common progenitor cells in wt and *ΔIG* E15 fetal liver (n=5). (**E** and **F**) Frequency in TNC (E) and absolute numbers (F) of mature lineage cells in wt and *ΔIG* E15 fetal liver (n=4). (**G**) Absolute numbers of LSK cells and CD93^{+} HSCs in wt, mat *ΔIG*, pat *Dlk1* KO and double mutant E15 fetal liver (n=2). (**H** and **I**) Frequency in TNC of common progenitor cells (H) and mature lineage cells (I) in wt and mat *ΔGtl2* E15 fetal liver (n=3). Error bars, SEM. Scale bars, 5 mm. ns, not significant; $*p < 0.05$.

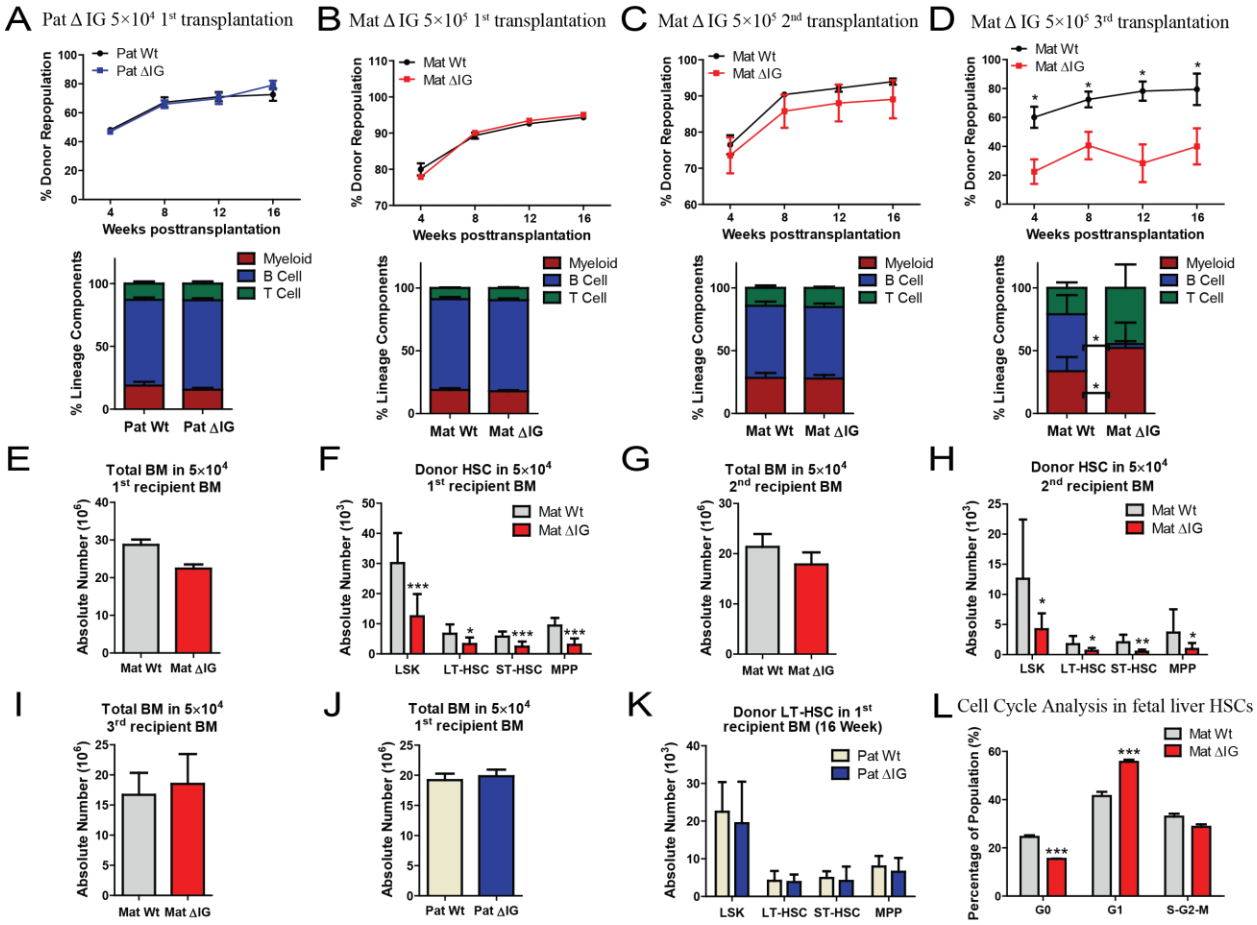

Figure S3. Loss of Maternal, but not Paternal, Imprinting at *Dlk1-Gtl2* Locus Impaired Long-term Reconstitution Capacity of Fetal Liver HSCs, Related to Figure 3. (**A**) 5×10^4 wt or pat *ΔIG* fetal liver cells were transplanted with 1×10^5 rescue cells into irradiated recipients. PB was analyzed for percent donor repopulation at the indicated number of weeks posttransplantation (top panels) and for percent mature donor-derived B, T, and myeloid cells (bottom panels) (n=10). (**B-D**) 5×10^5 wt or mat *ΔIG* fetal liver cells were transplanted with 1×10^5 rescue cells into irradiated recipients. At 16 wks posttransplantation, BM isolated from 1st recipients was transplanted into 2nd recipients and, at 16 wks after 2nd transplant, from 2nd into 3rd recipients at a dosage of 1×10^6 cells per mouse. PB was analyzed for percent donor repopulation at the indicated number of weeks after 1st, 2nd, and 3rd transplant (top panels) and for percent mature donor-derived B, T, and myeloid cells (bottom panels) (n=10). (**E** and **F**) At 16 wks posttransplantation, absolute numbers of total BM cells (E) and HSPCs (F) in the BM from 1st recipients with 5×10^4 wt or mat *ΔIG* fetal liver cells (n=10). (**G** and **H**) At 16 wks posttransplantation, absolute numbers of total BM cells (G) and HSPCs (H) in the BM from 2nd recipients with 5×10^4 wt or mat *ΔIG* fetal liver cells (n≥8). (**I**) At 16 wks posttransplantation, absolute numbers of total BM cells from 3rd recipients with 5×10^4 wt or mat *ΔIG* fetal liver cells (n≥4). (**J** and **K**) At 16 wks posttransplantation, absolute numbers of total BM cells (J) and HSPCs (K) in the BM from 1st recipients with 5×10^4 wt or pat *ΔIG* fetal liver cells (n=10). (**L**) Cell cycle analysis of E15 wt or mat *ΔIG* fetal liver $CD93^+$ HSCs (n≥3). Error bars, SD. $*p < 0.05$; $**p < 0.01$; $***p < 0.001$.

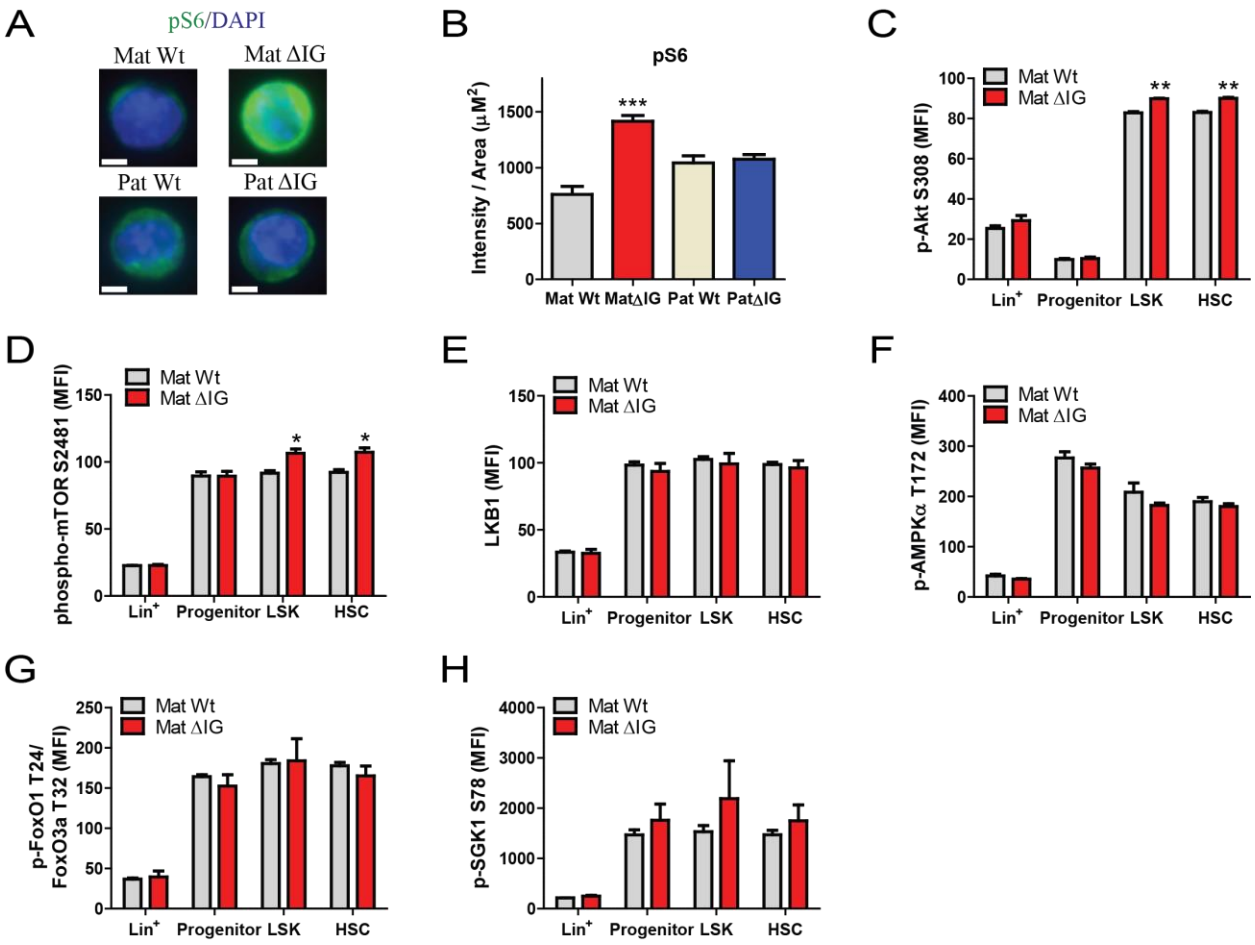

Figure S4. Hyperactivation of PI3K-mTOR Pathway in mat *ΔIG* Fetal Liver HSPCs, Related to Figure 4 and Table S7. (**A** and **B**) Representative image (A) and quantification (B) of staining intensity of LSK cells sorted from wt and *ΔIG* fetal livers for p-S6$^{S235/236}$ (n≥72). (**C-H**) MFI of p-Akt^{S308} (C), p-mTOR^{S2481} (D), LKB1 (E), p-AMPKα^{T172} (F), p-FoxO1^{T24}/FoxO3a^{T32} (G) and p-SGK1^{S78} (H) in wt and mat *ΔIG* fetal liver HSCs (n=2-3). Error bars, SEM or SD (**B**). Scale bars, 5 μm. ∗p < 0.05; ∗∗∗p < 0.001.

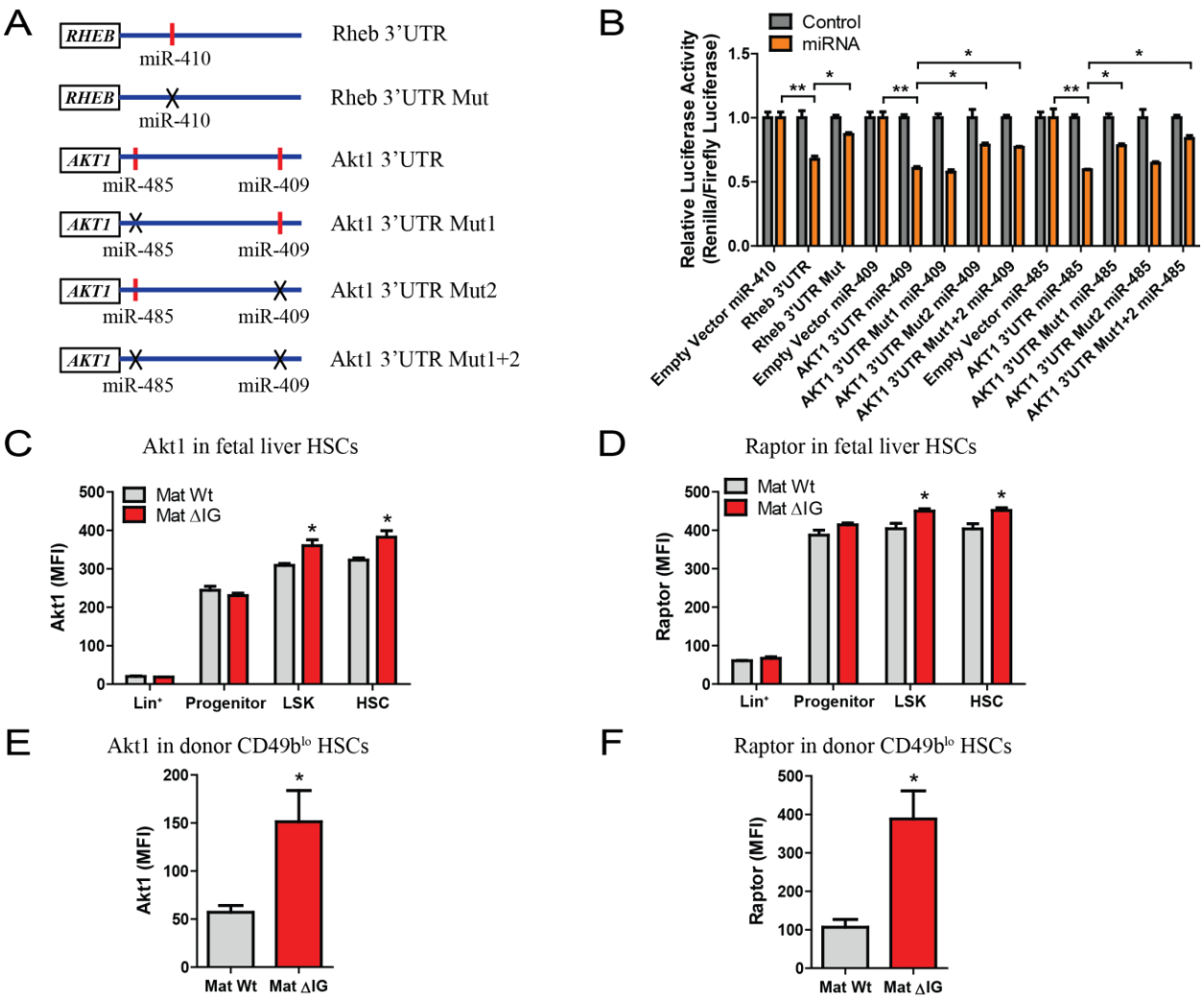

Figure S5. miRNAs in the *Dlk1-Gtl2* Locus Repressed Multiple Components of PI3K-mTOR Pathway, Related to Figure 5 and Table S6, S7. (**A**) Schematic diagram shows mutations of miRNA binding sites on 3'UTRs of RHEB and AKT1. (**B**) Luciferase reporter assays shows repression of miRNAs was abrogated by mutations of cognate miRNA binding sites (n=2). (**C** and **D**) Expression of AKT1 (C) and RPTOR (D) determined by intracellular flow cytometry in wt and mat *ΔIG* fetal liver cells (n=2). (**E** and **F**) Expression of AKT1 (E) and RPTOR (F) determined by intracellular flow cytometry in donor CD49b^{lo} HSCs from BM of 3rd recipients (n≥4). Error bars, SEM or SD (**E** and **F**). $*p < 0.05$; $**p < 0.01$.

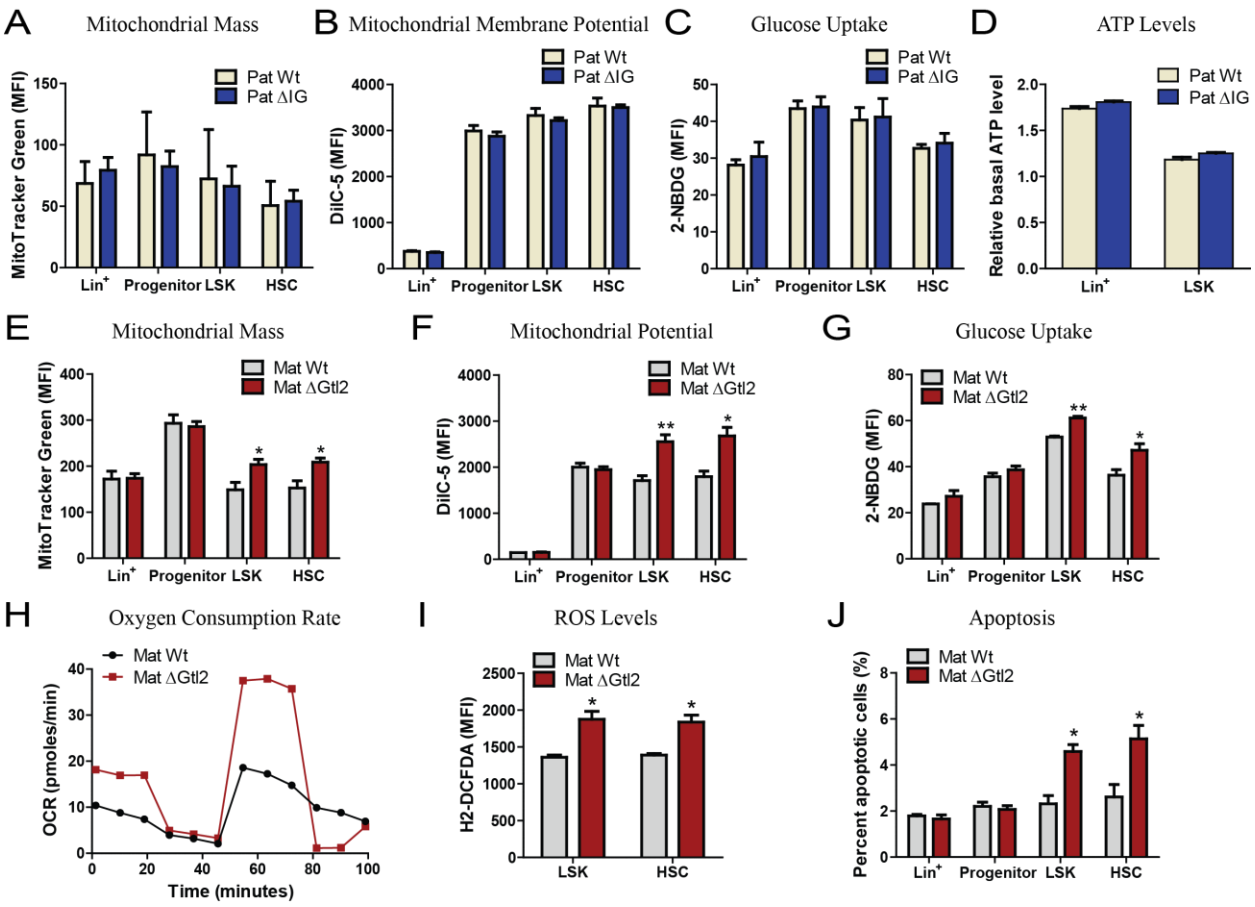

Figure S6. Loss of *Gtl2 per se*, whereas not pat *ΔIG*, Enhanced Mitochondrial Biogenesis, Metabolic Activity and Increased ROS Levels in HSCs, Related to Figure 6. (**A**) Mitochondrial mass of wt and pat *ΔIG* cells assayed by MitoTracker Green staining (n=2). (**B**) Mitochondrial membrane potential of wt and pat *ΔIG* cells assayed by DilC5 staining (n=2). (**C**) Glucose uptake of wt and pat *ΔIG* cells assayed by 2-NBDG (n=2). (**D**) The relative basal ATP levels of wt and pat *ΔIG* cells (n=2). (**E**) Mitochondrial mass of wt and mat *ΔGtl2* cells assayed by MitoTracker Green staining (n=3). (**F**) Mitochondrial membrane potential of wt and mat *ΔGtl2* cells assayed by DilC5 staining (n=3). (**G**) Glucose uptake of wt and mat *ΔGtl2* cells assayed by 2-NBDG (n=3). (**H**) Oxygen consumption rate of wt and mat *ΔGtl2* cells assayed by Seahorse assay. (**I**) ROS levels of wt and mat *ΔGtl2* cells assayed by H2-DCFDA (n=3). (**J**) Percentage of apoptotic cells in wt and mat *ΔGtl2* cells assayed by Annexin V and 7-AAD staining (n=3). Error bars, SEM. $*p < 0.05$; $**p < 0.01$.

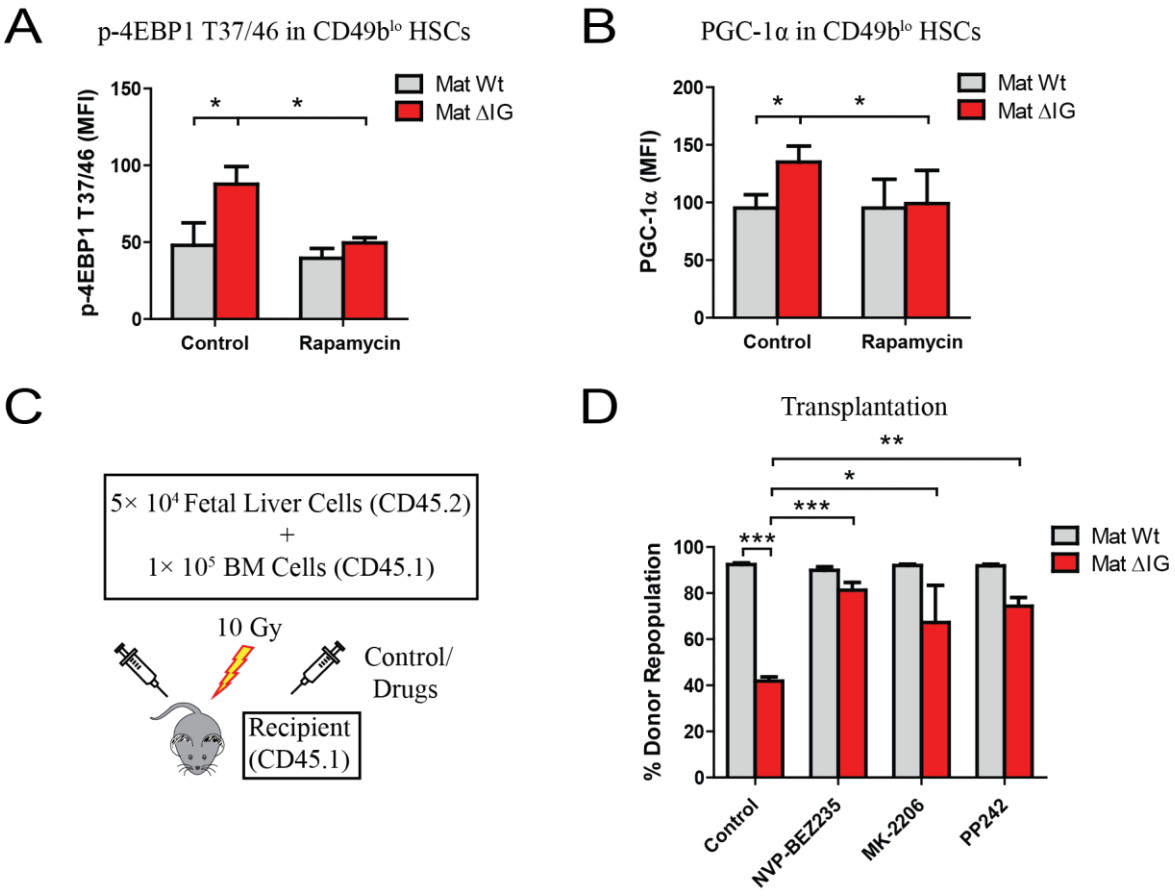

Figure S7. Pharmacological Inhibition of PI3K-mTOR Pathway Partially Rescued HSC Deficiency in mat *ΔIG* Mutant, Related to Figure 7 and Table S7. (**A** and **B**) MFI of p-4E-BP1$^{T37/46}$ (A) and PGC-1α (B) expression within donor CD49b^{lo} HSCs from BM of mice with rapamycin administration at 12 wks posttransplantation (n≥4). (**C**) Scheme for administration of PI3K-mTOR pathway inhibitors. (**D**) Repopulation assay for administration of PI3K-mTOR pathway inhibitors at 16 wks posttransplantation (n=6). Error bars, SD. ∗p < 0.05; ∗∗p < 0.01; ∗∗∗p < 0.001.

SUPPLEMENTAL TABLES

Table S1. Purification of Hematopoietic Cell Populations Used in This Study, Related to Figures 1, 2, 4, 5, Figure S1 and Supplemental Experimental Procedures.

Table S2. FPKMs of All Transcripts Used in This Study by High-throughput RNA-seq, Related to Figures 1, 2, 4, 5, Figure S1 and Supplemental Experimental Procedures.

Table S3. LncRNA Fingerprints Unique to Each Hematopoietic Cell Type, Related to Figure 1.

Table S4. GO Analysis Using Slim-term List and Biological Process in the Mat *ΔIG*/Mat Wt, Related to Figure 4.

Table S5. Small RNA Seq Identified 15 miRNAs and 10 snoRNAs in Both Fetal Liver HSC and Adult HSCs, Related to Figure 5.

Table S6. Sequences of the Oligonucleotides for miRNAs, Plasmid Construction, and qRT-PCR Analysis, Related to Figures 2, 5, Figure S5 and Supplemental Experimental Procedures.

Table S7. List of Proteins Tested by Antibodies and Characteristics of the Corresponding Antibodies Used, Related to Figures 4, 5, 6, 7, Figures S4, S5, S7 and Supplemental Experimental Procedures.

SUPPLEMENTAL EXPERIMENTAL PROCEDURES

Poly-A^+ RNA Seq

RNA sequencing was performed as previously described (Sugimura et al., 2012; Venkatraman et al., 2013). Four hematopoietic stem and progenitor cells (HSPCs) ($CD49b^{lo}$ LT-HSC, $CD49b^{hi}$ IT-HSC, ST-HSC and MPP) (Benveniste et al., 2010), adult LSK cells (Okada et al., 1992), 4 committed progenitors (CLP, CMP, GMP and MEP) (Akashi et al., 2000; Kondo et al., 1997) and 9 mature lineage cells (B cell (Coffman and Weissman, 1981; Wortis et al., 1995), T cell (Cron et al., 1989), NK cell (Koo et al., 1986), dendritic cell (Grouard et al., 1996; Zhou and Tedder, 1996), macrophage (Weischenfeldt and Porse, 2008), monocyte, granulocyte (Longhi et al., 2009), megakaryocyte (Tiedt et al., 2007) and nucleated erythrocyte (Socolovsky et al., 2001)) were collected by fluorescence-activated cell sorting (FACS) from the bone marrow (BM) of at least four 8-12-week-old C57BL/6J mice (biological replicates). Fetal liver LSK cells were separated by FACS from E15.0 fetal live cells (Kawamoto et al., 1997). Total RNA was isolated from these cells using the TRIzol (Life Technologies) according to the manufacturer's instructions. RNA concentrations and RNA integrity were determined by Agilent RNA 6000 Pico Kit on BioAnalyzer 2100 (Agilent Technologies). Poly-A^+ RNA was then isolated and libraries were constructed from approximately 10-100 ng of total RNA for each sample using the TruSeq RNA sample preparation kit v2 (Illumina). The fragment size in the generated library ranged from 220 to 500 bps with a peak at 350 bps. A total of 10 fmol library fragments were loaded to cBot to generate clusters, followed by sequencing on an Illumina HiSeq 2000 to produce 19-66 million paired-end 100 bp reads for samples from adult mice and single-end 50bp reads for samples from E15 fetal livers. Poly-A^+ RNA seq data were submitted to Array Express E-MTAB-2923 (4 HSPCs and macrophage) and E-MTAB-3079 (4 committed progenitors, 8 lineage cells, adult LSK and 2 fetal liver LSK cells).

All the samples were trimmed to 70bp, except for the two 50bp single-end fetal liver samples. Reads were aligned to UCSC mm10 using Tophat 2.0.9 (Trapnell et al., 2009), Ensembl 75 GTF, parameters "--no-coverage-search". A Cufflinks 2.1.1 (Trapnell et al., 2010) run was made for each sample, with no GTF, to discover novel transcripts; parameters used were "-u --max-bundle-frags 3000000".

In our analyses, FPKMs had to have a pseudocount added, prior to taking log2, to prevent infinites. These are referred to as "Adjusted" FPKMs. We set the detectability floor for FPKMs to be 2^{-10}, based on the $\log_2$-FPKM density histograms. Cufflinks FPKMs $< 2^{-10}$ were replaced with zero. This allowed us to use 2^{-11}, or half the detectability threshold, as the pseudocount. This is equivalent to using 0.5 as the pseudocount in read-count-based analyses. Genes with FPKM ≥ 1 in at least one sample were considered "expressed". The value of 1 was taken from $\log_2$-FPKM densities, as it approximates the saddle point between the modes.

Novel lncRNAs Identification Pipeline

(1) Filtering

Novel transcripts were extracted from each sample and merged into a single set of models using Cuffcompare. We used multiple filtering strategies to identify novel loci and discarded the loci if they met any one of these criteria: (1) had only one exon; (2) had a maximum transcript length < 200bp, (3) had exonic overlap with any Ensembl 75 (Flicek et al., 2014) or UCSC known-gene

(Sep 27 2014) models (Karolchik et al., 2014). Using these stringent filtering strategies, 4782 novel transcripts were retained which formed 2082 novel loci.

(2) Annotation

The final model set was re-quantitated with Cufflinks, using prior parameters. Coding potential of all models was evaluated using NCBI-blastx against Swissprot, Pfam-A, and Pfam-B, restricting to subjects from mouse, rat, human, and chimp. Transcripts were remapped from mm10 into rn5, hg38, and panTro4 using liftOver, and any transcripts for which all mappable exons aligned to the same chromosome were converted to fasta and analyzed with PhyloCSF (Lin et al., 2011), parameters "29mammals --removeRefGaps --orf=ATGStop -f3". Finally, ORFs were extracted from three frames of every transcript, and were defined as starting with ATG and ending with a stop codon, or otherwise at the end of the transcript sequence.

Many transcripts failed to blast, or failed to return PhyloCSF scores due to lack of ORFs. In this case, their metrics were given the "worst" values possible. In the case of unblastable transcripts, the lowest observed blast score of 20 and highest observed E-value of 10 were conferred. In case of PhyloCSF failures, the lowest observed score of -457 was conferred.

We evaluated a variety of metrics from the blastx results to see which best distinguished Ensembl protein-coding from Ensembl noncoding transcripts. For clarity's sake, in further analysis, transcripts considered "noncoding" were only taken from obligatory noncoding loci. Pseudogenes were labeled as such, and noncoding transcripts from coding loci were ignored. In the end, we chose three metrics for classification, relying only on hits to mouse subjects. Hits to human subjects were as discriminative as mouse in several metrics, but never better, and rat and chimp metrics were too low to be useful. We found that the strongest distinguisher of coding versus noncoding was blast score, where a cutoff of 76.7 correctly classified 91.9% of coding transcripts (above cutoff) and 91.9% noncoding transcripts (below cutoff). The next most discriminative metrics were Pfam A and B E-values, for which thresholds were 0.0178 and 0.045, respectively. These cutoffs correctly classified 84.9% coding and noncoding (Pfam-A), and 73.5% coding and noncoding (Pfam-B).

We also compared the PhyloCSF scores of all coding, noncoding, and pseudogene Ensembl transcripts, and found the three distributions to be too redundant for an obvious score cutoff, certainly not the score of zero which theoretically distinguishes coding from noncoding. A previous study has reported good results for lncRNA classification using a maximum score of 100 (Alvarez-Dominguez et al., 2014). In our Ensembl data, this corresponds to a sensitivity of 98.4% but specificity of only 45.7% for noncoding status, or alternatively, a 54.3% false positive rate but only a 1.6% false negative rate. Considering that, in our hands, a score above 100 essentially guaranteed protein-coding status, and we also retained this threshold as a criterion.

(3) Biotype Assignment

Thus novel transcripts were considered "likely noncoding" if they had: ORF length < 100, Swissprot blastx score < 76.7, Pfam-A blastx E-value > 0.0178, Pfam-B blastx E-value > 0.045, and PhyloCSF score < 100; there were 2458. Transcripts with ORF length < 100 and at least one of the other criteria were considered "putative noncoding" (1005). Reciprocally, transcripts failing all 5 criteria were considered "likely coding" (22), and otherwise those with ORF length > 100 and PhyloCSF score > 100 were considered "putative coding" (102). The remainder were considered "unclassified" (1195). Finally, as many of our novel Cuffcompare loci contained multiple transcripts, locus-level classifications were taken as the highest-ranked classification of any

transcript in the locus, the rankings being “likely coding” > “putative coding” > “unclassified” > “putative noncoding” > “likely noncoding”. At the locus level, there were 10 “likely coding”, 24 “putative coding”, 442 “unclassified”, 416 “putative noncoding”, and 1190 “likely noncoding” assignments.

Fingerprint lncRNA Analysis

Tissue specificity (TS) scores per gene were calculated as previously described (Cabili et al., 2011), using $\log_2$ adjusted FPKMs. To prevent minor differences in FPKM distributions between samples from dominating tissue-specificity scoring, we first performed between-samples quantile normalization using the limma (Smyth, 2004) package in R. All samples were normalized to the ST-HSC sample, which had the clearest bimodality in FPKMs. We then found that a TS cutoff of 0.4 provided a good tradeoff between the number of genes which were specific to one sample, i.e. having a score >= 0.4 in only one sample, and the evenness of fingerprint gene number across samples, as measured by coefficient of variation. There were 461 lncRNA fingerprint genes, of which 375 were novel loci.

RNA-seq Data Analysis from Fetal Liver LSK Samples

Differentially expressed genes for the Mat *ΔIG*/Mat Wt comparison were based on two criteria: fold-change ≥ 2 and mean expression ≥ 1. These strategies yielded 991 upregulated and 941 downregulated genes. These two gene sets were further compared for GO term enrichment using a custom GO-slim list of 32 terms, comparing each list to the rest of the genome. Terms, and the genome, were taken from the geneontology.org database, Jan 2014 release.

Small RNA Seq and Data Analysis

20,000 each of four adult HSPCs (CD49b^{lo} LT-HSC, CD49b^{hi} IT-HSC, ST-HSC and MPP) were collected by FACS from the BM of at least four 8-10-week-old C57BL/6J mice (biological replicates). 50,000 each of four fetal liver LSK cells were isolated by FACS from E15.0 fetal livers of mat *ΔIG*, pat *ΔIG*, and their littermate controls. Total RNA was then isolated from these cells using the TRIzol (Life Technologies) according to the manufacturer’s instructions. RNA concentrations and RNA integrity were determined by Agilent RNA 6000 Pico Kit on BioAnalyzer 2100 (Agilent Technologies). Small RNA sequencing libraries were then constructed using the TruSeq Small RNA sample preparation kit (Illumina) according to the manufacturer’s instructions. cDNA fragments of 140-300 bp from these libraries were selected by gel purification. The integrity and concentrations of cDNA libraries were determined by Agilent high sensitivity DNA analysis kit on BioAnalyzer 2100 (Agilent Technologies) and then sequenced on an Illumina HiSeq2000 sequencer. The resulting 50 bp single-end reads were quality-checked with FastQC (http://www.bioinformatics.babraham.ac.uk/projects/fastqc/), trimmed to 70 bp due to quality, and aligned to UCSC mm10 with TopHat 2.0.9 (Trapnell et al., 2009), with custom parameter "--no-coverage-search", using Ensembl 73 gene models. Small RNA seq data were submitted to Array Express E-MTAB-3080.

Small RNA samples were trimmed using trimmomatic (Bolger et al., 2014), parameters “ILLUMINACLIP:adapters.fa:2:14:7 MINLEN:10”, where adapters.fa holds the Illumina adapters and RNA PCR primers found in the file "contaminants_list.txt" as distributed by FastQC 0.10.1 (http://www.bioinformatics.babraham.ac.uk/projects/fastqc/). Trimmed reads were aligned with Bowtie2 2.1.0 (Langmead and Salzberg, 2012), parameters "--very-sensitive-local". For track files, reads were aligned to mm10; for quantitation, reads were aligned to a custom ncRNA fasta.

This fasta contained all rRNA and small ncRNA species from Ensembl 73, including miRNA, snRNA, snoRNA, Mt_rRNA, Mt_tRNA, and all misc_RNA with housekeeping functions, also all tRNAScan-SE (Schattner et al., 2005) tRNA predictions for mm10, and the 45kb ribosomal complete repeating unit (gi|511668571|tpg|BK000964.3) from NCBI. Read counts per ncRNA were manually converted to RPKMs (reads per kilobase of transcript per million reads mapped).

Cell Lines and Cell Culture

HEK293T and mouse MEF cell lines used in this study were obtained from the American Type Culture Collection (ATCC) and cultured as recommended. All procedures involving human cell line HEK293T and lentiviral methodologies were approved by the Institutional Biosafety Committee (IBC) of Stowers Institute for Medical Research (SIMR).

Flow Cytometry

For adult mice, HSPCs, progenitor, and lineage cells were harvested from BM (femur and tibia) and peripheral blood. Red blood cells were lysed using a 0.16 M ammonium chloride solution. For cell surface phenotyping, a lineage cocktail (Lin) was used, including CD3, CD4, CD8, CD11b (Mac-1), Gr1, CD45R (B220), IgM and Ter119 (eBioscience). Monoclonal antibodies against Sca-1, c-Kit, CD34, Flk2, CD49b, CD127 (IL-7Rα), CD16/32 (FcγRII/III), NK1.1, CD11c, CD83, CD115 (CFMS), F4/80, CD71, CD45, CD45.1 and CD45.2 were also used where indicated and summarized in Supplemental Table S1.

For fetal liver HSC phenotype analysis, fetal livers were dissected from E15.0 embryos and then gently digested using 18 gauge needles (BD Biosciences) in 1mg/ml collagenase solution (Sigma-Aldrich) at 37˚C for 5 min. Then cells were filtered through 40μm cell strainer (Falcon) and centrifuged at 300g for 5min, followed by treatment with 0.16 M ammonium chloride solution at 37˚C for 5 min to lyse red blood cells. A different lineage cocktail (Lin) was used in fetal liver cells, including CD3, CD4, CD8, Gr1, B220, IgM and Ter119. Antibodies against Sca-1, c-Kit, CD38 and CD93 were used where indicated.

Total numbers of cells from E15.0 fetal livers or recipient BM were counted by Cell Lab Quanta (Beckman Coulter) and 1-5 million cells were stained with HSC markers and then resuspended in 1ml of warm PBS. To measure mitochondrial mass, cells were incubated with 20 nM MitoTracker Green (Invitrogen) at 37˚C for 30 min. To measure mitochondrial membrane potential, cells were incubated with 50 nM DilC-5 (Invitrogen) at 37˚C for 15-30 min. To determine glucose uptake, cells were incubated with 10 μM 2-NBDG (Invitrogen) at 37 ˚C for 1 h. To measure ROS levels, cells were incubated with 50 nM H2-DCFDA (Invitrogen) at 37˚C for 15 min. Cell sorting and analysis were performed using a MoFlo (Dako), InFlux Cell Sorter (BD Biosciences), and/or CyAn ADP (Dako). Data analysis was performed using FlowJo software.

Rapamycin, NAC and PI3K-mTOR Inhibitors Treatment

Rapamycin (LC Laboratories) was reconstituted in absolute ethanol at 10 mg/ml and diluted in 5% Tween-80 (Sigma-Aldrich) and 5% PEG-400 (Fisher Scientific). One week posttransplantation, recipient mice received rapamycin (4 mg/kg) or control by intraperitoneal injection every day for 12 weeks. NAC (Sigma-Aldrich) was dissolved in distilled water at 1 mg/ml. One week posttransplantation, mice were fed with control or NAC water for 16 weeks. NVP-BEZ235 (LC Laboratories, free base) was formulated in NMP/polyethylene glycol (PEG) 300 (10/90, v/v) at 4 mg/ml. One week posttransplantation, mice were orally gavaged with 40 mg/kg NVP-BEZ235 daily, 5 days a week for 3 weeks. PP242 (LC Laboratories, free base) was formulated in PEG 400

at 6 mg/ml. One week posttransplantation, mice were orally gavaged with 60 mg/kg PP242 twice a day for 5 days. MK-2206 2HCl (Selleck Chemicals) was formulated in 30% Captisol (Captisol Technology) in water at 1 mg/ml. One week posttransplantation, mice were orally gavaged with 10 mg/kg MK-2206 twice a day for 7 days.

Transplantation Studies

For competitive reconstitution assays, 5×10^4 or 5×10^5 E15.0 total fetal liver cells, or 150 sorted LSK/CD93$^+$ fetal liver cells from *IG-DMR* (CD45.2) mice were transplanted intravenously together with 1×10^5 or 2×10^5 Ptprc (CD45.1) rescue BM cells into lethally irradiated (10 Gy) Ptprc recipient mice, respectively. Baytril water was given to recipient mice 3 days before irradiation, and continued for another 2 weeks after irradiation.

The *in vivo* competitive repopulation unit (CRU) assay (Szilvassy et al., 1990) was performed by transplantation of a series (5,000, 15,000 and 50,000) of diluted donor-derived fetal liver cells from wt or *Gtl2* KO mice with a fixed number of 1×10^5 rescue cells (CD45.2) into groups of ten lethally irradiated (10 Gy) recipient mice (CD45.1). CRU frequency was measured using ELDA (Extreme limiting dilution assay) software (Hu and Smyth, 2009), in which successful engraftment was defined as the presence of a distinct CD45.2$^+$ CD45.1$^-$ population ($\geq$1%) above a background set by parallel analysis of animals transplanted with only rescue BM (Haug et al., 2008). For 2nd and 3rd transplantations, original transplant recipients were sacrificed. After dissecting BM from femur and tibia, we then transplanted mouse-to-mouse at a dosage of 1×10^6 cells per mouse.

For transplantation assay rescued by overexpression of miRNAs in *Gtl2* locus, 5,000 LSK cells were sorted from E15.0 wt and mat *ΔIG* mutant fetal livers (CD45.2) and cultured in StemSpan media (Stemcell Technologies) supplemented with 10ng/ml recombinant mouse stem cell factor (SCF, Peprotech) and 20ng/ml recombinant mouse thrombopoietin (TPO, Peprotech) as previously described (Perry et al., 2011). After 18 hours, cells were infected with either pSico-control or a pool of lentiviruses with overexpression of 10 highly expressed miRNAs in the *Gtl2* locus (miR-134, miR-136, miR-409, miR-410, miR-411, miR-433, miR-485, miR-540, miR-541, and miR-673) in the presence of 4 μg/mL polybrene (Sigma). 48 hours after infection, 5×10^4 MNCs with 2×10^5 (CD45.1) Ptprc rescue BM cells were transplanted into CD45.1 recipient mice.

For rapamycin, NAC, or PI3K-mTOR inhibitors rescue transplantation, 150 LSK/CD93$^+$ fetal liver HSCs (CD45.2) or 5×10^4 E15.0 total fetal liver cells from mat *ΔIG* mutant or control embryos along with 2×10^5 (CD45.1) Ptprc rescue BM cells were transplanted into CD45.1 recipient mice. One week after transplantation, recipient mice received rapamycin (4 mg/kg) or vehicle control by intraperitoneal injection every day for 12 weeks (Yilmaz et al., 2006); recipient mice were fed with NAC water for 16 weeks, or were orally gavaged with NVP-BEZ235, PP242, or MK-2206, respectively.

Each transplanted group consisted of five to ten recipients. Donor-derived engraftment was determined every 4 weeks posttransplantation, followed by collection of peripheral blood, red blood cell lysis and staining with CD45.1 (recipient) and CD45.2 (donor) antibodies. Multilineage reconstitution was determined on CyAn ADP (Dako) by CD3, B220 (for T and B lymphoid, respectively) and Gr1, Mac-1 (for myeloid) gating on donor (CD45.21) cells.

Fetal Liver Tissue Genotyping

Tails were dissected from E15 wt and *ΔIG* mutant embryos. Then DNA was extracted and PCR was performed using Extract-N-Amp™ Tissue PCR Kit (Sigma-Aldrich) according to the manufacturer's instruction. PCR products were electrophoresed on 1.5% agarose gels at 120V for

30 min and taken images. Primers used for genotyping were the same as previous reports (Lin et al., 2003; Takahashi et al., 2009).

qRT-PCR

To measure expression levels of genes in *Dlk1-Gtl2* locus in fetal liver cells, 20,000 each of Lin^+, Progenitors (Lin^- $Sca1^-$ $cKit^+$), LSK (Lin^- $Sca1^+$ $cKit^+$), $CD38^{lo}$ LSK and $CD38^{hi}$ LSK cells were directly sorted into 500 μl Trizol (Ambion, Austin TX) from E15.0 wt or mat *ΔIG* mutant fetal livers. RNA was extracted and treated at 37˚C for 30 min with 2 μl RNase-free DNase-1 (2 U/μl; Ambion), followed by reverse transcription and pre-amplification using ABI Reverse Transcription and Taqman PreAmp Kit (Applied Biosystems) according to the manufacturer's instruction. TaqMan gene expression assays (Applied Biosystems) were performed on triplicate samples using a 7900HT fast real-time PCR system (Applied Biosystems). Data were normalized relative to *β-actin*.

The mitochondrial DNA copy numbers were carried out as previously described (Nakada et al., 2010). Briefly, genomic and mitochondrial DNA was extracted using DNeasy Blood and Tissue kit (QIAGEN), and mtDNA copy numbers were quantified by qRT-PCR using 7900HT fast real-time PCR system (Applied Biosystems). The serial numbers of TaqMan probes are listed in Supplemental Table S6.

miRNA Oligos and Plasmid Cloning

miRNA mimics and scramble control RNAs were purchased from Genepharma (Shanghai, China). The full-length sequences of 3'UTRs were amplified from genomic DNA of B6 BM cells and subcloned into the reporter plasmid psiCHECK2 (Promega). All the 3'UTR mutant constructs of AKT1 and RHEB were generated using the QuickChange II XL site-directed mutagenesis kit (Stratagene) to delete the seed sequences and confirmed by DNA sequencing. For overexpression of 10 highly expressed miRNAs in the *Gtl2* locus (miR-134, miR-136, miR-409, miR-410, miR-411, miR-433, miR-485, miR-540, miR-541, miR-673), DNA fragments about 300bp upstream and downstream around miRNA locus were cloned individually from genomic DNA of B6 BM cells into pSico-EF1α-IRES2-EGFP lentiviral vector. All the sequences of miRNAs mimics, primers for plasmid cloning are detailed in Supplemental Table S6.

Lentivirus Production and Transduction

The pSico-EF1α-IRES2-EGFP-miRNA expressed and pSico-control lentiviruses were generated by transfection of pSico constructs together with the psPAX2 and pMD2.G plasmids at a ratio of 10:7.5:2.5 into HEK293T cells using calcium phosphate transfection. The virus particles were harvested 48, 72, and 96 hours after transfection, filtered by 0.45 micrometers filter unit (Millipore), and then centrifuged at 18,000 RPM, 4˚C for 2 hours. Mouse MEF cells or sorted LSK cells were infected with recombinant lentivirus-transducing units in the presence of 4 μg/mL polybrene (Sigma). 48 hours after infection, cells were collected for analysis or transplantation.

Western Blotting

Cells were collected and homogenized in RIPA buffer (20mM Tris pH 8.0, 150mM NaCl, 0.1% SDS, 0.5% DOC, 0.5% triton X-100) with protease inhibitors cocktail (Roche). Cell lysates equivalent to 50-100g of total protein were fractionated on 4%-20% SDS-polyacrylamide gradient gels (Bio-Rad) and transferred to nitrocellulose membranes (0.2 μm, Bio-Rad). Membranes were blocked with 5% BSA at room temperature for 1 hour and then incubated overnight with anti-

AKT1, anti-RPTOR (Cell Signaling Technology), anti-beta-ACTIN (Novus Biologicals). Detection was performed by using HRP-conjugated antibodies and Luminata Forte chemiluminescence (Millipore). All the antibody information is listed in Supplemental Table S7.

Immunostaining

Immunostaining was performed as described previously (Zhang et al., 2003). Briefly, cells were sorted onto Poly-L-lysine coating slides, fixed with chilled methanol for 10 min, blocked and stained for p-Akt^{S473}, p-mTOR^{S2448} or p-S6$^{S235/236}$. Images were taken on Axiomager Z1 (Zeiss) with AxioVision 4.7.2.0, and staining intensity per image was quantified by ImageJ program. The characteristics of these antibodies are listed in Supplemental Table S7.

***In Vivo* ATP Measurement**

20,000 LSK or Lin^+ cells were rapidly sorted from E15.0 fetal livers into PBS. Immediately after centrifuge, cell pellet was resuspended in boiled cell lysis buffer (100 mM Tris, 4 mM EDTA, pH 7.75) and incubated at 100˚C for 2 min. Samples were then centrifuged at 10,000g for 1 min and the supernatant was transferred into a fresh tube and kept on ice. ATP concentration was measured using the ATP Determination kit (Invitrogen). Each ATP sample was measured in triplicate.

Transmission Electron Microscopy

Sorted cells were collected in gel (or agarose) and fixed in 2.5% glutaraldehyde for 2 hours at room temperature. Then sample was washed 3 times (10 min each) in PBS and post-fixed in aqueous 1% OsO_4, 1% $K_3Fe(CN)_6$ for one hour at room temperature. After 3 PBS washes, the sample was dehydrated through a graded series of 30-100% ethanol, propylene oxide then infiltrated and embedded in epoxy resin, and polymerized for 48 hours at 60 °C. Ultrathin (about 60 nm) sections were cut and collected on copper grids, stained with 2% uranyl acetate and 1% lead citrate. Sections were viewed and photographed using a FEI transmission electron microscope operated at 80kV.

Seahorse Assay

Sorted LSK cells (100,000 per well) were attached to the bottom of a XF96 Tissue Culture Plate (Seahorse Bioscience) coated with BD Cell-Tak Cell Adhesive, and oxygen consumption rate (OCR) was measured using the Seahorse XF96 instrument (Seahorse Biosciences). Respiration was measured under basal conditions, in the presence of the mitochondrial inhibitor oligomycin (2 μM), mitochondrial uncoupler FCCP (5 μM), and respiratory chain inhibitor antimycin and rotenone (1 μM).

Cell Cycle Analysis

Cell cycle analysis of HSCs was performed with FITC Mouse Anti-Human Ki67 Set (BD Pharmingen) following the manufacturer's instruction. The fetal liver cells and donor HSCs were then incubated with 0.1 mg/mL DAPI or Sytox Red (Invitrogen), respectively, for 10 min at room temperature, followed by flow cytometric analysis with InFlux Cell Sorter (BD Biosciences).

Apoptosis Analysis

Apoptosis was measured by staining freshly harvested fetal liver cells with lineage, stem and progenitor markers, followed by Annexin-V-FITC and 7-AAD staining (BD Bioscience).

SUPPLEMENTAL REFERENCES

Akashi, K., Traver, D., Miyamoto, T., and Weissman, I.L. (2000). A clonogenic common myeloid progenitor that gives rise to all myeloid lineages. Nature *404*, 193-197.

Alvarez-Dominguez, J.R., Hu, W., Yuan, B., Shi, J., Park, S.S., Gromatzky, A.A., van Oudenaarden, A., and Lodish, H.F. (2014). Global discovery of erythroid long noncoding RNAs reveals novel regulators of red cell maturation. Blood *123*, 570-581.

Benveniste, P., Frelin, C., Janmohamed, S., Barbara, M., Herrington, R., Hyam, D., and Iscove, N.N. (2010). Intermediate-term hematopoietic stem cells with extended but time-limited reconstitution potential. Cell stem cell *6*, 48-58.

Bolger, A.M., Lohse, M., and Usadel, B. (2014). Trimmomatic: a flexible trimmer for Illumina sequence data. Bioinformatics *30*, 2114-2120.

Cabili, M.N., Trapnell, C., Goff, L., Koziol, M., Tazon-Vega, B., Regev, A., and Rinn, J.L. (2011). Integrative annotation of human large intergenic noncoding RNAs reveals global properties and specific subclasses. Genes & development *25*, 1915-1927.

Coffman, R.L., and Weissman, I.L. (1981). B220: a B cell-specific member of th T200 glycoprotein family. Nature *289*, 681-683.

Cron, R.Q., Gajewski, T.F., Sharrow, S.O., Fitch, F.W., Matis, L.A., and Bluestone, J.A. (1989). Phenotypic and functional analysis of murine CD3+,CD4-,CD8- TCR-gamma delta-expressing peripheral T cells. J Immunol *142*, 3754-3762.

Flicek, P., Amode, M.R., Barrell, D., Beal, K., Billis, K., Brent, S., Carvalho-Silva, D., Clapham, P., Coates, G., Fitzgerald, S., *et al.* (2014). Ensembl 2014. Nucleic acids research *42*, D749-755.

Grouard, G., Durand, I., Filgueira, L., Banchereau, J., and Liu, Y.J. (1996). Dendritic cells capable of stimulating T cells in germinal centres. Nature *384*, 364-367.

Haug, J.S., He, X.C., Grindley, J.C., Wunderlich, J.P., Gaudenz, K., Ross, J.T., Paulson, A., Wagner, K.P., Xie, Y., Zhu, R., *et al.* (2008). N-cadherin expression level distinguishes reserved versus primed states of hematopoietic stem cells. Cell stem cell *2*, 367-379.

Hu, Y., and Smyth, G.K. (2009). ELDA: extreme limiting dilution analysis for comparing depleted and enriched populations in stem cell and other assays. Journal of immunological methods *347*, 70-78.

Karolchik, D., Barber, G.P., Casper, J., Clawson, H., Cline, M.S., Diekhans, M., Dreszer, T.R., Fujita, P.A., Guruvadoo, L., Haeussler, M., *et al.* (2014). The UCSC Genome Browser database: 2014 update. Nucleic acids research *42*, D764-770.

Kawamoto, H., Ohmura, K., and Katsura, Y. (1997). Direct evidence for the commitment of hematopoietic stem cells to T, B and myeloid lineages in murine fetal liver. International immunology *9*, 1011-1019.

Kondo, M., Weissman, I.L., and Akashi, K. (1997). Identification of clonogenic common lymphoid progenitors in mouse bone marrow. Cell *91*, 661-672.

Koo, G.C., Dumont, F.J., Tutt, M., Hackett, J., Jr., and Kumar, V. (1986). The NK-1.1(-) mouse: a model to study differentiation of murine NK cells. J Immunol *137*, 3742-3747.

Langmead, B., and Salzberg, S.L. (2012). Fast gapped-read alignment with Bowtie 2. Nature methods *9*, 357-359.

Lin, M.F., Jungreis, I., and Kellis, M. (2011). PhyloCSF: a comparative genomics method to distinguish protein coding and non-coding regions. Bioinformatics *27*, i275-282.

Lin, S.P., Youngson, N., Takada, S., Seitz, H., Reik, W., Paulsen, M., Cavaille, J., and Ferguson-Smith, A.C. (2003). Asymmetric regulation of imprinting on the maternal and paternal chromosomes at the Dlk1-Gtl2 imprinted cluster on mouse chromosome 12. Nature genetics *35*, 97-102.

Longhi, M.P., Trumpfheller, C., Idoyaga, J., Caskey, M., Matos, I., Kluger, C., Salazar, A.M., Colonna, M., and Steinman, R.M. (2009). Dendritic cells require a systemic type I interferon response to mature and induce CD4+ Th1 immunity with poly IC as adjuvant. The Journal of experimental medicine *206*, 1589-1602.

Luo, M., Jeong, M., Sun, D., Park, H.J., Rodriguez, B.A., Xia, Z., Yang, L., Zhang, X., Sheng, K., Darlington, G.J., *et al.* (2015). Long non-coding RNAs control hematopoietic stem cell function. Cell stem cell *16*, 426-438.

Nakada, D., Saunders, T.L., and Morrison, S.J. (2010). Lkb1 regulates cell cycle and energy metabolism in haematopoietic stem cells. Nature *468*, 653-658.

Okada, S., Nakauchi, H., Nagayoshi, K., Nishikawa, S., Miura, Y., and Suda, T. (1992). In vivo and in vitro stem cell function of c-kit- and Sca-1-positive murine hematopoietic cells. Blood *80*, 3044-3050.

Perry, J.M., He, X.C., Sugimura, R., Grindley, J.C., Haug, J.S., Ding, S., and Li, L. (2011). Cooperation between both Wnt/{beta}-catenin and PTEN/PI3K/Akt signaling promotes primitive hematopoietic stem cell self-renewal and expansion. Genes & development *25*, 1928-1942.

Schattner, P., Brooks, A.N., and Lowe, T.M. (2005). The tRNAscan-SE, snoscan and snoGPS web servers for the detection of tRNAs and snoRNAs. Nucleic acids research *33*, W686-689.

Smyth, G.K. (2004). Linear models and empirical bayes methods for assessing differential expression in microarray experiments. Statistical applications in genetics and molecular biology *3*, Article3.

Socolovsky, M., Nam, H., Fleming, M.D., Haase, V.H., Brugnara, C., and Lodish, H.F. (2001). Ineffective erythropoiesis in Stat5a(-/-)5b(-/-) mice due to decreased survival of early erythroblasts. Blood *98*, 3261-3273.

Sugimura, R., He, X.C., Venkatraman, A., Arai, F., Box, A., Semerad, C., Haug, J.S., Peng, L., Zhong, X.B., Suda, T., *et al.* (2012). Noncanonical Wnt signaling maintains hematopoietic stem cells in the niche. Cell *150*, 351-365.

Szilvassy, S.J., Humphries, R.K., Lansdorp, P.M., Eaves, A.C., and Eaves, C.J. (1990). Quantitative assay for totipotent reconstituting hematopoietic stem cells by a competitive repopulation strategy. Proceedings of the National Academy of Sciences of the United States of America *87*, 8736-8740.

Takahashi, N., Okamoto, A., Kobayashi, R., Shirai, M., Obata, Y., Ogawa, H., Sotomaru, Y., and Kono, T. (2009). Deletion of Gtl2, imprinted non-coding RNA, with its differentially methylated region induces lethal parent-origin-dependent defects in mice. Human molecular genetics *18*, 1879-1888.

Tiedt, R., Schomber, T., Hao-Shen, H., and Skoda, R.C. (2007). Pf4-Cre transgenic mice allow the generation of lineage-restricted gene knockouts for studying megakaryocyte and platelet function in vivo. Blood *109*, 1503-1506.

Trapnell, C., Pachter, L., and Salzberg, S.L. (2009). TopHat: discovering splice junctions with RNA-Seq. Bioinformatics *25*, 1105-1111.

Trapnell, C., Williams, B.A., Pertea, G., Mortazavi, A., Kwan, G., van Baren, M.J., Salzberg, S.L., Wold, B.J., and Pachter, L. (2010). Transcript assembly and quantification by RNA-Seq reveals unannotated transcripts and isoform switching during cell differentiation. Nature biotechnology *28*, 511-515.

Venkatraman, A., He, X.C., Thorvaldsen, J.L., Sugimura, R., Perry, J.M., Tao, F., Zhao, M., Christenson, M.K., Sanchez, R., Yu, J.Y., *et al.* (2013). Maternal imprinting at the H19-Igf2 locus maintains adult haematopoietic stem cell quiescence. Nature.

Weischenfeldt, J., and Porse, B. (2008). Bone Marrow-Derived Macrophages (BMM): Isolation and Applications. CSH protocols *2008*, pdb prot5080.

Wortis, H.H., Teutsch, M., Higer, M., Zheng, J., and Parker, D.C. (1995). B-cell activation by crosslinking of surface IgM or ligation of CD40 involves alternative signal pathways and results in different B-cell phenotypes. Proceedings of the National Academy of Sciences of the United States of America *92*, 3348-3352.

Yilmaz, O.H., Valdez, R., Theisen, B.K., Guo, W., Ferguson, D.O., Wu, H., and Morrison, S.J. (2006). Pten dependence distinguishes haematopoietic stem cells from leukaemia-initiating cells. Nature *441*, 475-482.

Zhang, J., Niu, C., Ye, L., Huang, H., He, X., Tong, W.G., Ross, J., Haug, J., Johnson, T., Feng, J.Q., *et al.* (2003). Identification of the haematopoietic stem cell niche and control of the niche size. Nature *425*, 836-841.

Zhou, L.J., and Tedder, T.F. (1996). CD14+ blood monocytes can differentiate into functionally mature CD83+ dendritic cells. Proceedings of the National Academy of Sciences of the United States of America *93*, 2588-2592.